SIMULTANEOUS MODELLING OF HEAT AND MOISTURE TRANSFER AND AIR-CONDITIONING SYSTEM IN BUILDINGS

Francis W. H. Yik†, C. P. Underwood‡ & W. K. Chow†
† Department of Building Services Engineering, The Hong Kong Polytechnic University, Hunghom, Kowloon, Hong Kong.
‡ Department of the Built Environment, University of Northumbria at Newcastle, Newcastle Upon Tyne, NE1 8ST, United Kingdom.

ABSTRACT
A simplified building heat and moisture transfer model has been developed and integrated with relevant air-conditioning system component models for simultaneous simulation of heat and moisture transfer at the building envelope, the indoor air-zone and the air-conditioning system. This model requires much less computational effort when compared with other more rigorous heat and moisture transfer modelling methods. The accuracy of prediction of the model has been compared with some experimental results. The model is outlined and the comparison tests on the integrated building and air-conditioning system model are described in this paper.

INTRODUCTION

Interstitial condensation may cause damages to building structures and increase building heat loss. Therefore, preventing its occurrence is essential for buildings in cold climate countries [e.g. 1,2]. Although interstitial condensation is a much lesser problem for buildings in warm and hot climate regions, moisture transfer in such buildings still requires serious attention. This is because most building materials are porous materials [3] within which moisture can stay in their internal voids and can migrate through the material when driving forces exist [4]. Under the influence of diurnal variations in outdoor weather conditions, internal heat and moisture loads, and in the indoor conditions given rise by intermittent operation of air-conditioning systems, porous building fabric materials can absorb moisture from the indoor air at certain time in the day and release the moisture back to the indoor air at a later time. This exhibits a moisture storage effect, similar to the thermal storage effect in sensible heat transfer in buildings. Significance of this effect has been studied both theoretically and experimentally [e.g. 5-11].

An appropriate mathematical model that can simultaneously simulate the coupled heat and moisture transfer in the building fabrics, the indoor air-zones and the performance of the air-condtioning systems will be a valuable tool to facilate the prediciton of the influence of the moisture storage effect on the indoor environment and on the operation of the air-conditioning systems in buildings. Experience of developing such a model [12-14] revealed that intensive computational efforts were required when a rigorous building heat and moisture transfer model was adopted. Such a model therefore is far from being practically usable for buildings and air-conditioning systems designs. A balance between the competing demands in rigours of the model, accuracy of prediction and the required computational effort has to be sought.

A simplified building heat and moisture transfer model has been developed [13] on the basis of the evaporation and condensation theory [15-17], which is regarded as one of the most promising methods for modelling heat and moisture transfer in building materials [18]. The model was derived on the assumption that vapour pressure would be the dominant driving potential for vapour moisture transfer, but would be related to and affected by the temperature in the material. Bulk transport of air and water vapour mixture due to a gradient of the total pressure of the gaseous mixture, i.e. the filtration flow, was neglected. The transport property of materials adopted in the model is called differential permeability [19] and a method to calculate this property was included [13]. Howells and Marshall's method [20] was adopted to solve the governing partial differential equations (PDEs) in which the PDEs were first approximated by a set of ordinary differential equations (ODEs) and then the Runge-Kutta-Mersion method [21] was applied to solve the ODEs.

Restricted by the assumptions made in its derivation, the model would be applicable only to materials that stay in pendular state [15]. Nonetheless, materials that are made from cement, such as concrete, which is the dominant building material in Hong Kong, belong to this class of materials. Due to the peculiar structure of the cement gel, the number of fine pores (approximately 15Å in size) that exist in concrete and cement plastering is extremely large, and the fine pores are disconnected by larger-sized capillary pores (approximately 500Å) [15]. Consequently, a significant amount of moisture can be detained in these materials under normal environmental conditions, but the liquid water stays primarily in the fine pores and are highly immobile. Thus, moisture transfer takes place predominantly by vapour

diffusion whilst the liquid moisture can transport from one region to another only after it has been evaporated into the vapour state. This matches with the assumptions that the material is under the pendular state and the evaporation and condensation theory applies.

This building and system heat and moisture transfer model is less demanding on computational effort when compared with other more rigorous heat and moisture transfer modelling methods [e.g. 15,16]. Its accuracy of prediction has been verified against Thomas and Burch's experimental results [22], and compared with measured indoor conditions in a simple office room. The model and the numerical solution method adopted are outlined and the model verification tests are described in this paper.

OUTLINE OF THE MODEL AND THE NUMERICAL SOLUTION METHOD

Governing equations

The differential permeability building heat and moisture transfer model was developed on the basis of the following two coupled partial differential equations (PDEs) (equations 1 & 2):

$$\left(\rho_l \frac{\partial \varepsilon_l}{\partial P_v}\right)\frac{\partial P_v}{\partial t} + \left(\rho_l \frac{\partial \varepsilon_l}{\partial T}\right)\frac{\partial T}{\partial t} = \mu \frac{\partial^2 P_v}{\partial x^2} + \frac{\partial \mu}{\partial x}\frac{\partial P_v}{\partial x} \qquad (1)$$

$$\left(-h_{fg}\rho_l \frac{\partial \varepsilon_l}{\partial P_v}\right)\frac{\partial P_v}{\partial t} + \left((\rho C_p)_B - h_{fg}\rho_l \frac{\partial \varepsilon_l}{\partial T}\right)\frac{\partial T}{\partial t} = k_B \frac{\partial^2 T}{\partial x^2} + \frac{\partial k_B}{\partial x}\frac{\partial T}{\partial x} \qquad (2)$$

These equations were derived on the basis of conservation of mass of liquid water and heat energy in an elemental layer of a slab of porous solid. The mass of water vapour in the pores was assumed to be negligible because the density of water vapour is very small when compared with the liquid. The one-dimensional heat and vapour moisture transfer, under the influence of a vapour pressure and a temperature gradient, and the latent heat of vaporization associated with changes in the liquid moisture content, were accounted for. Derivation of the governing PDEs has been described in detail in Ref. [13]. Compared with the more rigorous models due to Harmathy [15] and Huang [16], one less equation is involved in this model, because the filtration flow, which was found to account for only about 2% of the total moisture transport, was neglected [13,14].

The local volume fraction of liquid water (ε_l) in these PDEs were related to the corresponding vapour pressure (P_v) and temperature (T) through the use of the sorption isotherm for the porous material (in the form of equation 3). Sorption isotherm curves for many building materials can be found from the literature [e.g. 18,23], albeit the database needs to be expanded to cover a much wider range of materials that may be encountered in modern buildings.

$$\varepsilon_l = \varepsilon_l(RH)\big|_{T=const.}\ ;\ RH = P_v/P_{vs} \qquad (3)$$

Numerical solution methods

In the numerical solution process, equations 1 & 2 were first partially discretized, in the spatial dimension only, into a set of ordinary differential equations (ODEs). The semi-implicit scheme used by Howell and Marshall [20] was adopted to approximate the time derivatives [13] in this process. The procedures involved are briefly described, with reference to equation 4 (a short-hand form of equation 1) as follows:

$$a_{11}\frac{\partial P_v}{\partial t} + a_{12}\frac{\partial T}{\partial t} = c_{11}\frac{\partial^2 P_v}{\partial x^2} + c_{12}\frac{\partial P_v}{\partial x} \qquad (4)$$

i) The spatial derivatives of $P_v(x,t)$ were approximated by:

$$\frac{\partial P_v}{\partial x} \approx \frac{P_{v+} - P_{v-}}{2\Delta x}$$

$$\frac{\partial^2 P_v}{\partial x^2} \approx \frac{P_{v+} - 2P_v + P_{v-}}{(\Delta x)^2}$$

ii) Expressing the right hand side of equation 4 as a weighted sum of the above finite difference approximations evaluated at time t (time step n) and t+Δt (time step n+1), equation 4 becomes:

$$a_{11}\frac{\partial P_v}{\partial t} + a_{12}\frac{\partial T}{\partial t} = c_{11}\lambda\frac{\Delta P_{v+} - 2\Delta P_v + \Delta P_{v-}}{(\Delta x)^2} + c_{12}\lambda\frac{\Delta P_{v+} - \Delta P_{v-}}{2\Delta x} + c_{11}\frac{P_{v+}^n - 2P_v^n + P_{v-}^n}{(\Delta x)^2} + c_{12}\frac{P_{v+}^n - P_{v-}^n}{2\Delta x} \qquad (5)$$

where $\Delta P_v = P_v^{n+1} - P_v^n$, and likewise for ΔP_{v+} & ΔP_{v-}.

iii) The ΔP_v , ΔP_{v+} and ΔP_{v-} terms were each multiplied by $\Delta t/\Delta t$ to become:

$$\Delta t(\Delta P_v/\Delta t)\ ;\ \Delta t(\Delta P_{v+}/\Delta t)\ ;\ \Delta t(\Delta P_{v-}/\Delta t)$$

and were regarded respectively as:

$$\Delta t(dP_v/dt)\ ;\ \Delta t(dP_{v+}/dt)\ ;\ \Delta t(dP_{v-}/dt)$$

iv) Subsituting the above into equation 5 and, after re-arranging, an ordinary differential equation (equation 6) was obtained as an approximation of equation 4.

$$-\lambda\Delta t\left(\frac{c_{11}}{\Delta x^2}-\frac{c_{12}}{2\Delta x}\right)\frac{dP_{v-}}{dt}+\left(a_{11}+\lambda\Delta t\frac{2c_{11}}{\Delta x^2}\right)\frac{dP_v}{dt}$$

$$-\lambda\Delta t\left(\frac{c_{11}}{\Delta x^2}+\frac{c_{12}}{2\Delta x}\right)\frac{dP_{v+}}{dt}$$

$$=c_{11}\frac{P_{v+}^n-2P_v^n+P_{v-}^n}{\Delta x^2}+c_{12}\frac{P_{v+}^n-P_{v-}^n}{2\Delta x}-a_{12}\frac{dT}{dt} \quad (6)$$

The ODE approximation for equation 2 were likewise derived and equations for interior nodes, boundary nodes and interface nodes in a multi-layered wall or slab, are summarized in Table 1. The ODEs were then solved by using the Runge-Kutta-Merson (RKM) method [21], with the value of λ set to 1.0 (i.e. fully implicit). The merits of this method include:

- the fully implicit numerical scheme is stable;
- the time derivatives of the variables for the $(n+1)^{th}$ time step can be efficiently evaluated on the basis of calculated values for the n^{th} time step;
- the RKM method allows the error of each time step of calculation be estimated which can be used as the guideline to control the size of time-step to be used; and
- although an iterative procedure still needs to be used in solving the time derivatives, the coefficient matrices of the equations are tri-diagonal matrices and the efficient tri-diagonal matrix algorithm (TDMA) [21] can be employed in the solution process.

A comparison of the computational effort required has been carried out [13] on the basis of a reference case (a typical room in a concrete building) [12], which had been studied using a more rigorous heat and moisture transfer model that was developed from Huang's equations [16]. In that study [13], it was found that the simplified differential permeability model, in conjuction with the above numerical method, can reduce the computing time by a factor of 1/6 when the air-conditioning system were simulated simultaneously, and by a factor of 1/10 when no air-conditioning was assumed.

VERIFICATION OF MODEL PREDICTIONS

Heat and moisture transfer in a single slab of porous material

To verify that the differential permeability model can properly model heat and moisture transfer in porous materials, it was applied to repeat the simulation study done by Huang on drying of a piece of concrete slab [16] and to model Thomas and Burch's experiment on drying of a piece of gypsum board [22]. Reference conditions for the simulation studies are summarized in Tables 2 and 3. The results are compared with Huang's simulation and Thomas and Burch's experimental results in Figures 1 and 2 respectively.

It can be seen from Huang's predictions (Figure 1) that within the period simulated, the total gas pressure within the concrete slab rised, although this would gradually diminish later [16]. However, filtration flow was ignored in the differential permeability model. This may account for the deviations between the results predicted by the differential permeability model and Huang's results, particularly at the boundary nodes during the earlier part of the simulated period. In the later part, the two sets of results become much closer to each other. This shows that the simpler differential permeability model was capable of predicting heat and moisture transfer to an acceptable accuracy when compared with a more rigorous model.

In simulating Thomas and Burch's experiment on drying of a gypsum board sample, the surface convective mass transfer coefficient given in their paper [22] was used but the moisture transport property of the material, the differential permeability, was calculated using the following equation [13]:

$$\mu \approx \varepsilon_g D M_a M_v / M_g RT \quad (7)$$

Figure 2 shows that the results predicted by the differential permeability model are in good agreement with Thomas and Burch's experimental results.

Heat and moisture transfer in an intermittently air-conditioned office room

The model was applied to predict the indoor air conditions in an office room in the Hong Kong

Table 1 Summary of equations of the differential permeability model for a multi-layer wall or slab

A) For interior nodes

$$-\lambda\Delta t\left(\frac{c_{11}}{\Delta x^2}-\frac{c_{12}}{2\Delta x}\right)\frac{dP_{v-}}{dt}+\left(a_{11}+\lambda\Delta t\frac{2c_{11}}{\Delta x^2}\right)\frac{dP_v}{dt}-\lambda\Delta t\left(\frac{c_{11}}{\Delta x^2}+\frac{c_{12}}{2\Delta x}\right)\frac{dP_{v+}}{dt}=c_{11}\frac{P_{v+}^n-2P_v^n+P_{v-}^n}{\Delta x^2}+c_{12}\frac{P_{v+}^n-P_{v-}^n}{2\Delta x}-a_{12}\frac{dT}{dt}$$

$$-\lambda\Delta t\left(\frac{c_{21}}{\Delta x^2}-\frac{c_{22}}{2\Delta x}\right)\frac{dT_-}{dt}+\left(a_{22}+\lambda\Delta t\frac{2c_{21}}{\Delta x^2}\right)\frac{dT}{dt}-\lambda\Delta t\left(\frac{c_{21}}{\Delta x^2}+\frac{c_{22}}{2\Delta x}\right)\frac{dT_+}{dt}=c_{21}\frac{T_+^n-2T^n+T_-^n}{\Delta x^2}+c_{22}\frac{T_+^n-T_-^n}{2\Delta x}-a_{21}\frac{dP_v}{dt}$$

where $a_{11}=\rho_l\frac{\partial\varepsilon_l}{\partial P_v}$; $a_{12}=\rho_l\frac{\partial\varepsilon_l}{\partial T}$; $a_{21}=-h_{fg}\rho_l\frac{\partial\varepsilon_l}{\partial P_v}$; $a_{22}=(\rho C_p)_B-h_{fg}\rho_l\frac{\partial\varepsilon_l}{\partial T}$;

$c_{11}=\mu$; $c_{12}=\frac{\partial\mu}{\partial x}$; $c_{21}=k_B$; $c_{22}=\frac{\partial k_B}{\partial x}$

B) For boundary nodes

$$\left(a_{11}+\lambda\Delta t\frac{c_{12}}{\Delta x}\right)\frac{dP_v}{dt}-\left(\lambda\Delta t\frac{c_{12}}{\Delta x}\right)\frac{dP_{va}}{dt}=c_{12}\frac{P_{va}^n-P_v^n}{\Delta x}+d_1-a_{12}\frac{dT}{dt}$$

$$\left(a_{22}+\lambda\Delta t\frac{c_{22}}{\Delta x}\right)\frac{dT}{dt}-\left(\lambda\Delta t\frac{c_{22}}{\Delta x}\right)\frac{dT_a}{dt}=c_{22}\frac{T_a^n-T^n}{\Delta x}+d_2-a_{21}\frac{dP_v}{dt}$$

where $a_{11}=\rho_l\frac{\partial\varepsilon_l}{\partial P_v}$; $a_{12}=\rho_l\frac{\partial\varepsilon_l}{\partial T}$; $a_{21}=-h_{fg}\rho_l\frac{\partial\varepsilon_l}{\partial P_v}$; $a_{22}=(\rho C_p)_B-h_{fg}\rho_l\frac{\partial\varepsilon_l}{\partial T}$; $c_{12}=\frac{2\mu}{\Delta x}$; $c_{22}=\frac{2k_B}{\Delta x}$;

$d_1=\frac{2m_v''}{\Delta x}$; $d_2=\frac{2q''}{\Delta x}$

C) For interface nodes between adjacent layers

$$\left(-\lambda\Delta t\frac{\mu_-}{\Delta x_-}\right)\frac{dP_{v-}}{dt}+\left(a_{11}+\lambda\Delta t\left(\frac{\mu_-}{\Delta x_-}+\frac{\mu_+}{\Delta x_+}\right)\right)\frac{dP_v}{dt}-\left(\lambda\Delta t\frac{\mu_+}{\Delta x_+}\right)\frac{dP_{v+}}{dt}=-\mu_-\frac{P_v^n-P_{v-}^n}{\Delta x_-}+\mu_+\frac{P_{v+}^n-P_v^n}{\Delta x_+}-a_{12}\frac{dT}{dt}$$

$$\left(-\lambda\Delta t\frac{k_{B-}}{\Delta x_-}\right)\frac{dT_-}{dt}+\left(a_{22}+\lambda\Delta t\left(\frac{k_{B-}}{\Delta x_-}+\frac{k_{B+}}{\Delta x_+}\right)\right)\frac{dT}{dt}-\left(\lambda\Delta t\frac{k_{B+}}{\Delta x_+}\right)\frac{dT_+}{dt}=-k_{B-}\frac{T^n-T_-^n}{\Delta x_-}+k_{B+}\frac{T_+^n-T^n}{\Delta x_+}-a_{21}\frac{dP_v}{dt}$$

where $a_{11}=\rho_l\left(\frac{\partial\varepsilon_l}{\partial P_v}\right)_I$; $a_{12}=\rho_l\left(\frac{\partial\varepsilon_l}{\partial T}\right)_I$; $a_{21}=-\rho_l\left(h_{fg}\frac{\partial\varepsilon_l}{\partial P_v}\right)_I$; $a_{22}=(\rho C_p)_I-\rho_l\left(h_{fg}\frac{\partial\varepsilon_l}{\partial T}\right)_I$

and $\left(\frac{\partial\varepsilon_l}{\partial P_v}\right)_I=\frac{\Delta x_-}{2}\frac{\partial\varepsilon_{l-}}{\partial P_v}+\frac{\Delta x_+}{2}\frac{\partial\varepsilon_{l+}}{\partial P_v}$; $\left(\frac{\partial\varepsilon_l}{\partial T}\right)_I=\frac{\Delta x_-}{2}\frac{\partial\varepsilon_{l-}}{\partial T}+\frac{\Delta x_+}{2}\frac{\partial\varepsilon_{l+}}{\partial T}$;

$$\left(h_{fg}\frac{\partial\varepsilon_l}{\partial P_v}\right)_I=h_{fg-}\frac{\Delta x_-}{2}\frac{\partial\varepsilon_{l-}}{\partial P_v}+h_{fg+}\frac{\Delta x_+}{2}\frac{\partial\varepsilon_{l+}}{\partial P_v}\ ;$$

$$\left(h_{fg}\frac{\partial\varepsilon_l}{\partial T}\right)_I=h_{fg-}\frac{\Delta x_-}{2}\frac{\partial\varepsilon_{l-}}{\partial T}+h_{fg+}\frac{\Delta x_+}{2}\frac{\partial\varepsilon_{l+}}{\partial T}\ ;\ \&\ (\rho C_p)_I=\frac{\Delta x_-}{2}(\rho C_p)_{B-}+\frac{\Delta x_+}{2}(\rho C_p)_{B+}$$

Table 2 Conditions of Huang's simulation study on drying of a concrete slab [16]

Parameters	Sym.	Unit	Value
Thickness of slab	L	m	0.1
Height of slab	H	m	2.0
Dry porosity of solid	ε_0	$m^3\ m^{-3}$	0.3
Dry density of solid	ρ_0	$kg\ m^{-3}$	2600
Specific heat of solid	C_p	$J\ kg^{-1}\ K^{-1}$	879
Thermal conductivity of solid	k	$W\ m^{-1}\ K^{-1}$	1.4422
Initial moisture content	$\varepsilon_{l,ini}$	$m^3\ m^{-3}$	0.096
Initial temperature	T_{ini}	K	294.8
Mole fraction of water vapour in the ambient air at LHS	ϕ_1	$mol\ mol^{-1}$	0.0134
Mole fraction of water vapour in the ambient air at RHS	ϕ_2	$mol\ mol^{-1}$	0.003584
Ambient air temperature at LHS	T_1	K	303.0
Ambient air temperature at RHS	T_2	K	294.0
Enclosure temperature at LHS	T_{e1}	K	304.0
Enclosure temperature at RHS	T_{e2}	K	293.0

Table 3 Conditions of Thomas and Burch's experiment on drying of a slab of gypsum board [22]

Parameters	Sym.	Unit	Value
Thickness of slab	L	m	0.0132
Diameter of slab	d	m	0.18
Density of solid	ρ_0	$kg\ m^{-3}$	670
Specific heat of solid	C_p	$J\ kg^{-1}\ K^{-1}$	1089.4
Thermal conductivity of solid	k	$W\ m^{-1}\ K^{-1}$	0.1593
Initial moisture content	$\varepsilon_{l,ini}$	$m^3\ m^{-3}$	0.00529
Ambient air temperature	T_{amb}	K	297.0
Initial relative humidity of the ambient air	RH_{ini}	%	74
New relative humidity of the ambient air	RH_{amb}	%	26
Surface mass transfer coefficient	h_m	$kg\ m^{-2}\ Pa^{-1}\ s^{-1}$	$3.2x10^{-8}$

Polytechnic University and the predictions were compared with measured data (Figures 3 & 4). The room modelled was rectangular in shape (3m (W) × 3m (D) × 3m (H)), comprising a south facing concrete external wall with a window on it (3m (W) × 1.5m (H)), three internal partition walls, a carpeted floor and a false ceiling with acoustic tiles. Air-conditioning was provided by a fan-coil unit the performance of which was simulated by models of a cooling coil a control valve and an on/off controller.

In the measurement period, the room was unoccupied, the air-conditioning system and the lighting were turned on during the daytime and switched off during the nighttime on weekdays, and remained off throughout the day on weekends. In order to make the heat and moisture storage effects more prominent, and hence more easily measurable, a lower than normal indoor temperature was maintained during the air-conditioned periods, by setting the thermostat associated with the fan-coil unit at the lowest possible set-point (19°C). Details about the room and the air-conditioning system and, about the air-conditioning system component models, can be found from Ref. [14].

From Figures 3 & 4, it can be seen that the model predictions and the measured data are in reasonably good agreement in respect of the general variation patterns of the variables. However, the humidity ratio of the room air was underestimated during the air-conditioned periods and the indoor temperature was overestimated during the non-air-conditioned periods. Such deviations are somewhat expected because the model cannot completely account for the complicated and varied situations in a real building. Particularly, the effects of finishing materials at the walls, the floor and the ceiling, and the effects of other hygroscopic materials that were present in the room, such as furnitures, paper, etc., were ignored in the simulation. Also, disturbances to the operating conditions of the air-conditioning system (e.g. changes in chilled water supply temperature and pressure) were ignored. This comparison therefore may only be regarded as an illustration of the current simulation performance of the model rather than a validation of its prediction accuracy. Nonetheless, it shows that the model was capable of predicting the transient variations in indoor environmental conditions that were similar to actual conditions.

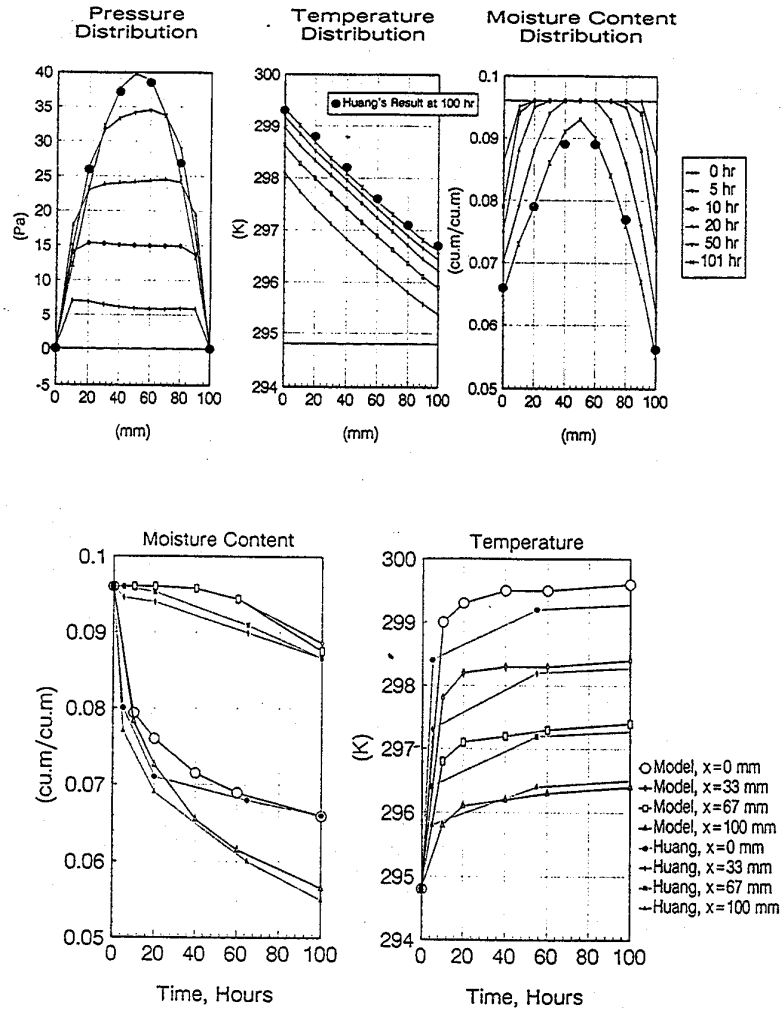

Figure 1 Comparison of simulation results between Huang's model [16] and the differential permeability model

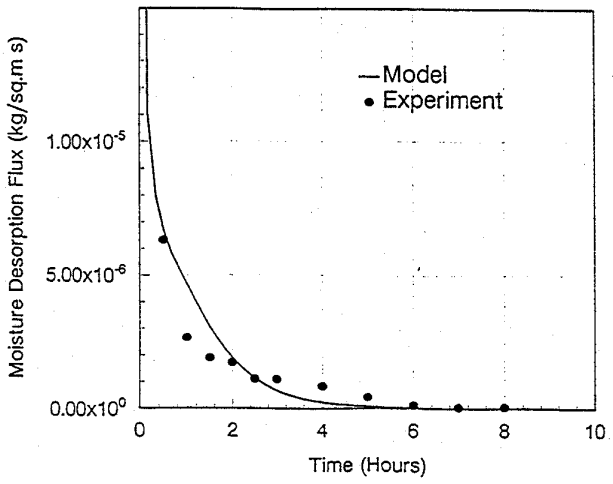

Figure 2 Comparison of moisture desorption rates from experiment (by Thomas & Burch [22]) and differential permeability model

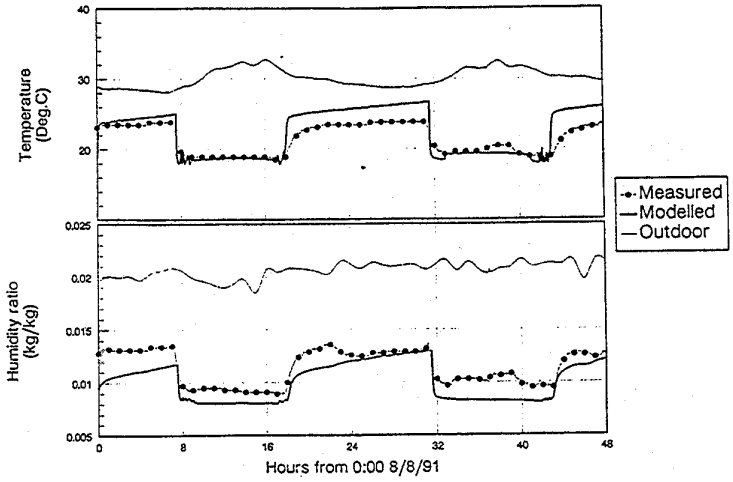

Figure 3 Comparison of predicted indoor conditions with measured data - I (from 8/8/91 - 9/8/91, weekdays)

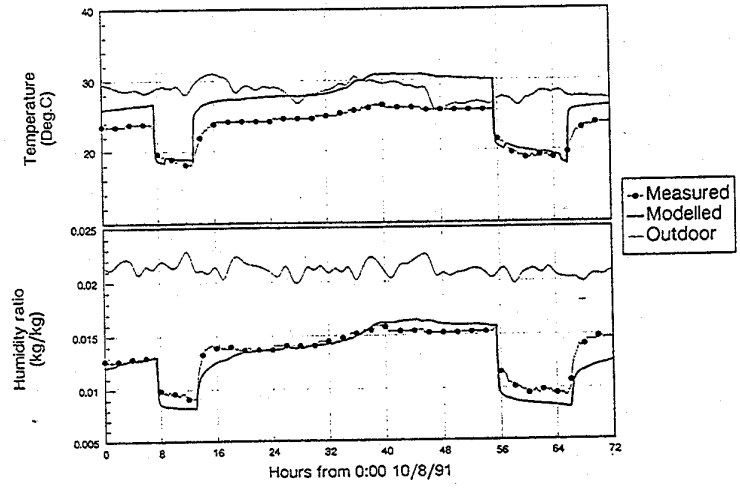

Figure 4 Comparison of predicted indoor conditions with measured data - II (from 10/8/91 - 12/8/91, included a weekend)

CONCLUSIONS

Predictions of the differential permeability model were in good agreement with predictions of a more rigorous model and with some experimental results, when applied to simulate single pieces of porous materials. The integrated building and air-conditioning system model, built from the differential permeability model, has been shown to be able to predict transient variations of indoor air conditions. However, this model requires improvements before it can more realistically and accurately simulate actual buildings and air-conditioning systems. This requires further work in several aspects, including producing more accurate heat and moisture transport properties for a large range of building materials, enhancing the modelling ability by including models for finishing materials, furnitures and other hygroscopic materials that would be found in buildings, and producing accurate experimental data for validation of the model. Work on these aspects is ongoing. Also, it is encouraging to note that research along these lines are being actively pursued by others [e.g. 24, 25].

REFERENCES

1 BRE (1972) Condensation, Building Research Establishment, UK.

2 Letherman, K. M. (1989) Condensation avoidance in layered structures: Synthesis of designs, *Building Services Engineering Research and Technology*, 10(1), The Chartered Institution of Building Services Engineers, UK.

3 Whiteley, P., Russman, H. D. and Bishop, J. D. (1977) *Porosity of building materials - a collection of published results*, Current Paper CP21/77, Building Reseach Establishment, UK.

4 Luikov, A. V. (1966) *Heat and mass transfer in capillary porous bodies*, Pergamon Press.

5 Tsuchiya, T (1980) Infiltration and indoor air temperature and moisture variation in a detached residence, *JSHASE* 54(11), Japan.

6 Kusuda, T (1983) Indoor humidity calculations, *ASHRAE Transactions* V.89, Pt.II, American Society of Heating, Refrigerating and Air-conditioning Engineers Inc., USA.

7 Miller, J. D. (1984) Development and validation of a moisture mass balance model for predicting residential cooling energy computation, *ASHRAE Transactions* V.90, Pt.IIB, American Society of Heating,

Refrigerating and Air-conditioning Engineers Inc., USA.

8 Fairey, P. W. & Kerestecioglu, A (1985) Dynamic modelling of combined thermal and moisture transport in buildings: Effects on cooling loads and space conditions, *ASHRAE Transactions* V.91, Pt.IIA, American Society of Heating, Refrigerating and Air-conditioning Engineers Inc., USA.

9 Shukuya, M & Saito, M (1990) Simulation of indoor air humidity using control volume heat and moisture balance method, Energy and Building, 14(1990), Elsevier, Sequoia.

10 Wong, S P W & Wang, S K (1990) Fundamentals of simultaneous heat and moisture transfer between the building envelop and the conditioned space air, *ASHRAE Transactions* V.96, Pt.II, American Society of Heating, Refrigerating and Air-conditioning Engineers Inc., USA.

11 Wong, S P W (1990) Simulation of simutaneous heat and moisture transfer by using the finite difference method and verified tests in a test chamber, *ASHRAE Transactions* V.96 Pt.I, American Society of Heating, Refrigerating and Air-conditioning Engineers Inc., USA.

12 Yik, F W H (1991) Dynamic modelling of indoor air humidity, *Proc. of Building Simulation '91 Conference, August, 1991, Nice, France*, The International Building Performance Simulation Association.

13 Yik, F W H (1993) A differential permeability model for simulating building heat and moisture transfer, Paper No. 65, *Proc. CLIMA 2000 Conf., London, Nov., 1993*, The Chartered Institution of Building Services Engineers, U.K.

14 Yik, F W H (1993) *Methodologies for simulating heat and moisture transfer in air-conditioned buildings in sub-tropical climates*, PhD Thesis, University of Northumbria at Newcastle, U.K.

15 Harmathy, T. Z. (1971) Moisture and heat transport with particular reference to concrete, Research Paper # 494, Division of Building Research, NRCC, Ottawa, Canada.

16 Huang, C L D (1979) Multi-phase moisture transfer in porous media subjected to temperature gradient, *Int. J. Heat Mass Transfer*, V.22.

17 Huang, C. L. D., Siang, H. H. and Best, C. H. (1979) Heat and moisture transfer in concrete slabs, *Int. J. Heat Mass Transfer*, V.22.

18 Kerestecioglu, A., Swami, M., Dabir, R., Razzaq, N. and Fairey, P. (1988), Theoretical and computational investigation of algorithms for simultaneous heat and moisture transport in buildings, Final Report to US DOE, FSEC-CR-191-88, Florida Solar Energy Centre, USA.

19 McLean, R C & Galbraith, G (1988) Interstitial condensation: applicability of conventional vapour permeability values, *Building Services Engineering Research and Technology*, 9(1), pp.29-34, The Chartered Institution of Building Services Engineers, UK.

20 Howells, P B & Marshall, H R (1981) A fast and accurate integration scheme for coupled stiff differential equations, *Proc. Int. Conf. Numerical Methods for Coupled Problems*, pp.45-49, Swansea: Pineridge Press.

21 Gear, C. W. (1971) *Numerical initial value problems in ordinary differential equations*, Prentice-Hall.

22 Thomas, W C & Burch, D M (1990) Experimental validation of a mathematical model for predicting water vapour sorption at interior building surfaces, *ASHRAE Trans.* V.96, Pt.1.

23 Hansen, K. K. (1986) *Sorption isotherms, a catalogue*, Building Materials Laboratory, The Technical University of Denmark.

24 Galbraith, G. and McLean, R. C. (1993) The determination of vapour and liquid transport coefficients as input to combined heat and mass transfer models, *Proc. IBPSA Building Simulation '93*, 3rd International Conference, Aldelaide, Australia, August, 1993.

25 Burch, D. M. (1993) Invitation to submit a research proposal on an ASHRAE research project - Moisture transfer in porous materials exposed to combined humidity and temperature gradients, Technical Committee 4.4, ASHRAE, USA.

NOMENCLATURE

C_p Specific heat (J kg^{-1} K^{-1})
D Diffusivity of water vapour in air (m^2 s^{-1})
ε_g Volume fraction in a porous medium occupied by the air and water vapour mixture (m^3 m^{-3})
ε_l Volume fraction of liquid water in a porous medium (m^3 m^{-3})
h_{fg} Heat of condensation/evaporation of water (J kg^{-1})
k Thermal conductivity (W m^{-1} K^{-1})
λ Weighting factor between the current and last time step value in discretization
μ Differential permeability (kg Pa^{-1} m^{-1} s^{-1} or s)
M Molecular weight (kg mol^{-1})
m_v'' Moisture flux (kg m^{-2} s^{-1})
P_v Partial pressure of water vapour (Pa)
q" Heat flux (W m^{-2})
ρ Density (kg m^{-3})
R Universal gas constant (J mol^{-1} K^{-1})
RH Relative humidity
T Temperature (K)
t Time (s)
x Spatial dimension in the direction of heat and moisture transfer (m)

Subscripts and Superscripts:

- The adjacent node to the left of the current node
+ The adjacent node to the right of the current node
a Dry air
B Bulk quantity of the porous medium
g Gaseous mixture of dry air and water vapour
l Liquid water
s Saturated condition
v Water vapour
n The n^{th} time step in the numerical solution process